

# Elastic-plastic analysis of the toughening mechanism in rubber-modified nylon: matrix yielding and cavitation

Takayuki Fukui, Yutaka Kikuchi and Takashi Inoue\*

Department of Organic and Polymeric Materials, Tokyo Institute of Technology,  
Meguro-ku, Tokyo 152, Japan

(Received 25 June 1990; revised 14 August 1990; accepted 7 September 1990)

The toughening mechanism of rubber-modified nylon is discussed in terms of elastic-plastic analysis of the tensile deformation of a two-dimensional model having five octahedral disc inclusions of rubber, facing each other with the disc-to-disc ligament thickness being kept constant. The rubber inclusion induces yielding of the matrix around it not only in the equatorial direction (perpendicular to the stretching direction), as expected from linear mechanics, but also in the  $\pm 45^\circ$  and  $\pm 135^\circ$  directions. At larger strains, the yielded zones expand further and eventually pervade over the whole matrix (strain  $\approx 0.3$ ). The massive yielding of the matrix is expected to result in a large amount of energy dissipation, and hence the material would be toughened. By similar analysis on a nylon/void system, the void is shown to play the same role for the toughening; however, it is less effective than rubber. The results suggest that a tougher material will be prepared when the interface between nylon and rubber is more strongly designed so that it is preserved from debonding (which corresponds to a transformation of the nylon/rubber system to the nylon/void system).

(Keywords: toughening mechanism; nylon; yielding; cavitation)

## INTRODUCTION

Rubber-toughened plastics, such as high impact polystyrene (HIPS) and acrylonitrile/butadiene/styrene (ABS) resin, constitute an important class of commercial thermoplastics. They are two-phase systems in which rubber particles with diameters of a few micrometres are dispersed in brittle polymer matrices. The toughening mechanism has been interpreted in terms of the craze and/or the shear band formation around the rubber particles<sup>1</sup>. Recent versions of rubber-toughened plastics, such as nylon/ethylene-co-propylene rubber (EPR), poly(phenylene oxide)/nylon/rubber and polycarbonate/poly(butylene terephthalate)/rubber, have ductile polymer matrices. They have similar morphologies to HIPS and ABS but exhibit much higher impact strengths.

Wu<sup>2</sup> investigated the toughening mechanism of the nylon/EPR system to show that the contribution of the craze and/or the shear band to the impact energy dissipation is minor and the energy dissipation is mostly by homogeneous yielding of the nylon matrix. Further he made a key observation<sup>3</sup> that a sharp brittle-tough transition occurs when the surface-to-surface interparticle distance,  $L$ , is reduced to a critical value  $L_c$ . Hence,  $L$  seems to be a single morphological parameter determining whether the rubber-modified nylon will be tough or brittle.

To understand the physical implication of  $L_c$ , we undertook a two-dimensional finite element method (FEM) analysis using a two-phase model in which an isolated rubber disc was embedded in a nylon matrix<sup>4</sup>. The FEM analysis showed that, as the applied stress is increased, the stress concentration occurs not only in the

equatorial ( $90^\circ$ ) but also in the polar ( $0^\circ$ ) and  $45^\circ$  directions around the rubber particle, resulting in massive yielding of the nylon matrix (Figure 1). Based on the FEM analysis, one may argue that if the neighbouring particles are taken into account (Figure 1), the stress fields around individual particles are expected to interfere or overlap with each other and hence more massive yielding is expected to pervade over the matrix as  $L$  is decreased. This is consistent with the phenomenological analysis by Wu<sup>5</sup>: the impact strength can be described by the three-dimensional percolation equation as a function of the volume fraction of a mechanical domain composed of the rubber particle (core) and a shell having a thickness of  $L_c/2$ .

Recently, another concept for rubber toughening has been proposed by Borggreve *et al.*<sup>6</sup> for the nylon/EPR system and by Hobbs *et al.*<sup>7</sup> for the poly(phenylene oxide)/nylon/rubber system. They suggested the

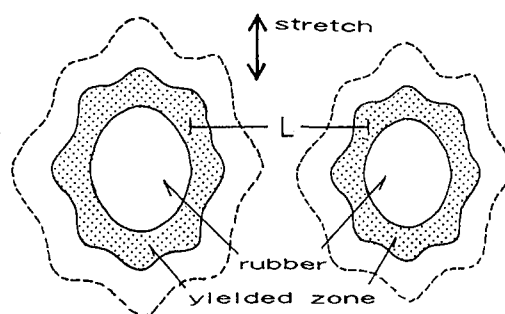


Figure 1 Evolution of a yielded zone of a nylon matrix around a rubber particle. The dashed line indicates the elastic limit. (Reproduced courtesy of The Society of Polymer Science, Japan)

\* To whom correspondence should be addressed

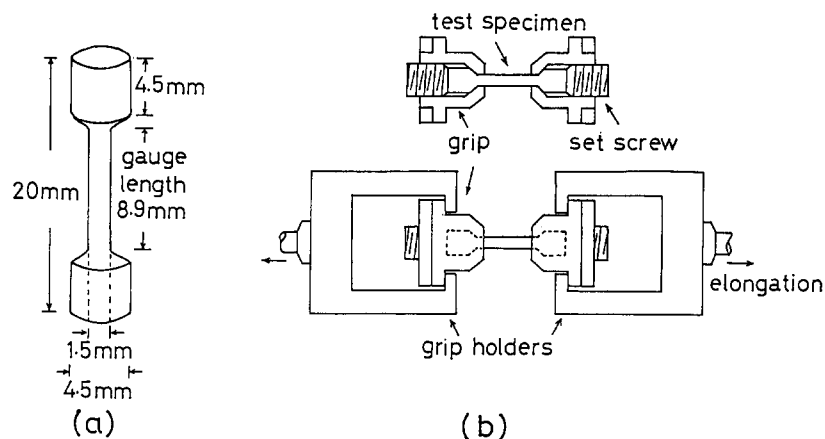


Figure 2 (a) Moulded dumb-bell specimen. (b) Gripping and clamping of the specimen for the tensile test

importance of cavitation, i.e. cavitation or void formation within rubber particles or at the interface plays an important role in toughening.

In this paper, we extend the FEM analysis to a many particle system in order to take into account the interference of stress fields between neighbouring particles, which was neglected in our previous discussion. We construct a modified FEM model with five rubber inclusions and carry out elastic-plastic analysis of the deformation. We also undertake a similar analysis on a nylon/void system having the same geometry, in relation to the cavitation mechanism. Both results are compared to justify the role of rubber particles in toughening.

## EXPERIMENTAL

For the elastic-plastic analysis by FEM, it is necessary to know the true stress-true strain behaviour of the component polymers. We prepared dumb-bell specimens of nylon and EPR and carried out the uniaxial tensile test.

The nylon 6 used was a commercial polymer (Novamid® 1010J, Mitsubishi Kasei Co. Ltd). EPR was modified with maleic anhydride to a level of 1 wt%\*. Each polymer was injection moulded into a miniature dumb-bell specimen using a Mini-Max injection moulder (model CS-183, Custom Scientific Instruments Inc.) set at 250°C. The dumb-bell specimen was rod-like as shown in Figure 2a, and was gripped and clamped as shown in Figure 2b. Tensile testing was carried out on a Mini-Max tensile tester (model CS-183TE, Custom Scientific Instruments Inc.) under a cross-head speed of 0.314 cm min<sup>-1</sup> at 25°C. During stretching, the diameter,  $D$ , of the specimen was observed using a video camera. After necking started, the diameter of the thinned region was assumed to be  $D$ . From the time variations of  $D$  and the load  $F$ , true stress,  $\sigma$ , and true strain,  $\epsilon'$ , were calculated:

$$\sigma = F/A = 4F/\pi D^2 \quad (1)$$

$$\epsilon' = \ln \epsilon = \ln(A_0/A) = 2 \ln(D_0/D) \quad (2)$$

where  $A$  is the cross-sectional area of specimen and the subscript 0 represents the unstretched state<sup>8</sup>. Thus the rod-type specimen provides a convenient method for estimating the variation of  $A$  with stretching by studying  $D$ .

\* To obtain the fine dispersion of EPR particles, EPR is usually modified with maleic anhydride to provide reaction sites on EPR chains

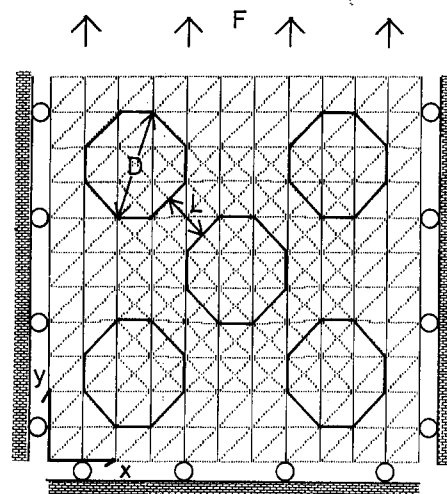


Figure 3 Two-dimensional FEM model

## FEM ANALYSIS

We constructed a FEM model with five octahedral disc inclusions of rubber, facing each other with the disc-to-disc ligament distance  $L$  being kept constant ( $L/D = 0.74$ ) as shown in Figure 3. Each element was assumed to have mechanical properties identical to those of the neat component polymer. That is, it was assumed that the element exhibits the same true stress-true strain curve observed for the component polymer. Poisson's ratio for rubber was assumed to be 0.49 and that for nylon equal to 0.30.

The computer program used for FEM calculation was a two-dimensional non-linear program (EPIC-IV) which can deal with elastic-plastic mechanics. Numerical calculations were carried out on a large-scale computer (Sun-3 Work Station, Sun-Microsystem Inc.).

The FEM model was uniaxially stretched in the  $y$ -direction under the plane-strain condition ( $\epsilon_z = 0$ ). Stress in the  $x$ ,  $y$  and  $z$  directions ( $\sigma_x$ ,  $\sigma_y$  and  $\sigma_z$ ) and a shear stress  $\tau_{xy}$  were calculated for each element as a function of bulk strain. The equivalent stress  $\bar{\sigma}$  defined by:

$$\bar{\sigma} = \{1/2[(\sigma_x - \sigma_y)^2 + (\sigma_y - \sigma_z)^2 + (\sigma_z - \sigma_x)^2 + 6\tau_{xy}^2]\}^{1/2} \quad (3)$$

was also calculated, where  $\bar{\sigma}$  is assumed to be a reduced tensile stress which is equivalent to the triaxial stress.

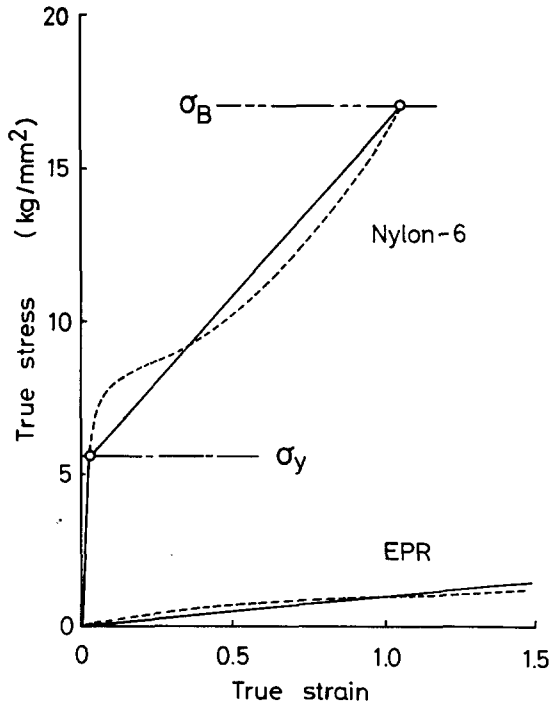


Figure 4 True stress-true strain curves of the constituent polymers and linear approximation (—)

RESULTS AND DISCUSSION

Figure 4 shows the true stress-true strain curves of nylon 6 and EPR. To simplify the FEM numerical calculation, the yield point was defined by the elastic limit and the curve was approximated and considered to be composed of two straight lines (Figure 4).

Figure 5 shows typical examples of the calculated results. Here the von Mises criterion for yielding was applied for the FEM elements, i.e. the matrix element was assumed to yield when  $\bar{\sigma}$  from equation (3) exceeded the yield stress  $\sigma_y$  on the true stress-true strain curve. The elements at which  $\bar{\sigma}$  is larger than  $\sigma_y$  are shaded. One can see that the rubber inclusion induces massive yielding of the nylon matrix around it and the number of yielded matrix elements increases with stretching. The number fraction of yielded elements,  $\phi_y$ , is shown as a function of bulk strain,  $\epsilon$ , in Figure 6. All the matrix elements are shown to be yielded at small strain;  $\phi_y = 1$  at  $\epsilon \geq 0.32$ . Thus, the modified model basically renders the same conclusion as the single particle model: massive yielding induced by the presence of rubber particles will result in a large amount of energy dissipation so that the two-phase material will be toughened.

For the nylon/void system, the results were similar to those in Figure 5 but the yielding of the matrix was slightly less than that for the nylon/rubber system. This is illustrated by a dashed line in Figure 6. One can see that yielding of the whole matrix has not been achieved even at  $\epsilon = 1$ .

Figure 7 shows the load  $F$  versus strain curve. The nylon/rubber system has a higher load than the void system. Combining the results of Figures 6 and 7, one may expect that the rubber inclusion will provide a more favourable situation for energy dissipation than the void inclusion. To confirm this, we now discuss the stress distribution and the fracture point.

Figure 8 shows the strain dependence of the equivalent

stress of the matrix elements facing the rubber phase in three directions;  $\theta = 0, 45$  and  $90^\circ$ , where  $\theta$  is the direction of the unstretched state. As expected by linear mechanics, the stress concentration is highest in the equatorial direction ( $\theta = 90^\circ$ ) in the small strain regime. At higher strain, a crossover takes place between  $\bar{\sigma} (\theta = 90^\circ)$  and  $\bar{\sigma} (\theta = 45^\circ)$ ;  $\bar{\sigma} (\theta = 45^\circ) > \bar{\sigma} (\theta = 90^\circ)$  at  $\epsilon > 0.05$ . This is a notable result from elastic-plastic analysis. The value of  $\bar{\sigma} (\theta = 45)$  in the nylon/void system is higher than that in the nylon/rubber system. This implies a more drastic (or more localized) stress concentration in the void system;

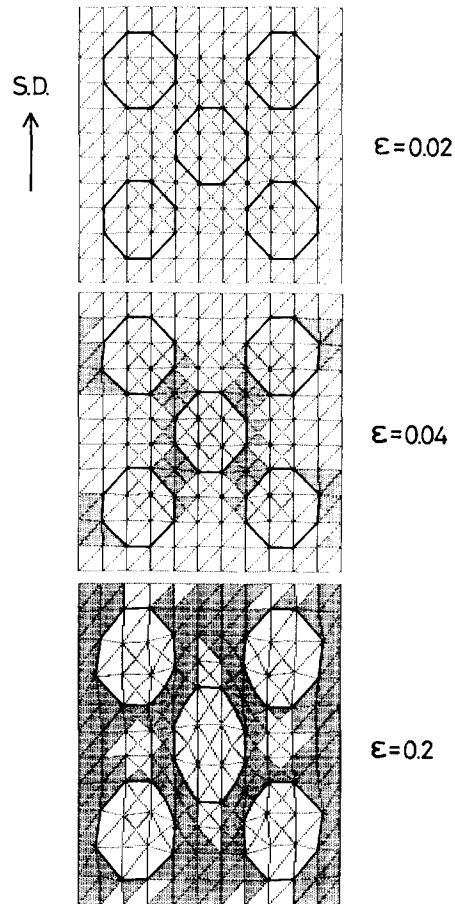


Figure 5 Deformation of the FEM model: simulated results for the nylon/rubber system. Yielded elements are shaded

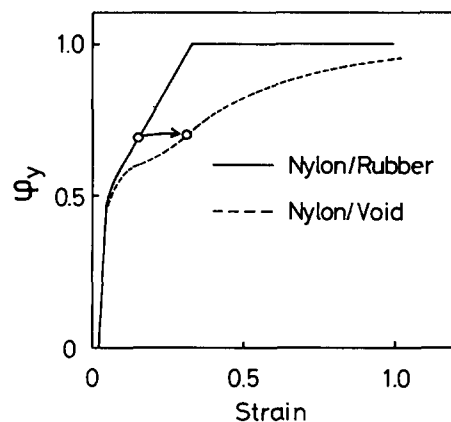


Figure 6 Variation of the number fraction of yielded matrix elements,  $\phi_y$ , with deformation

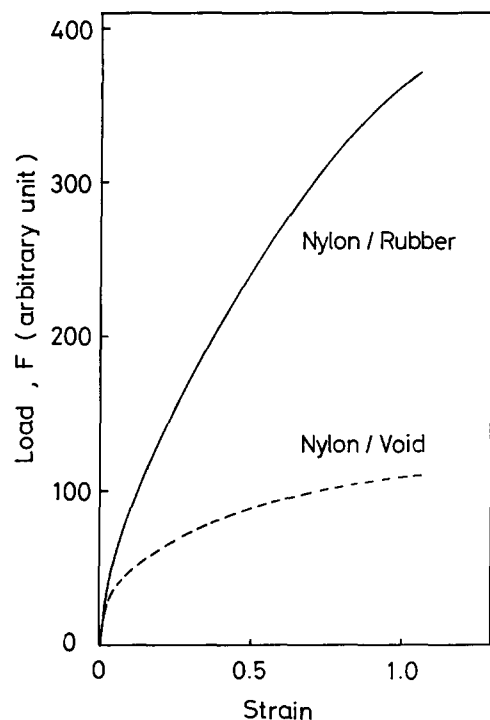


Figure 7 Load  $F$ -strain curves (see Figure 3)

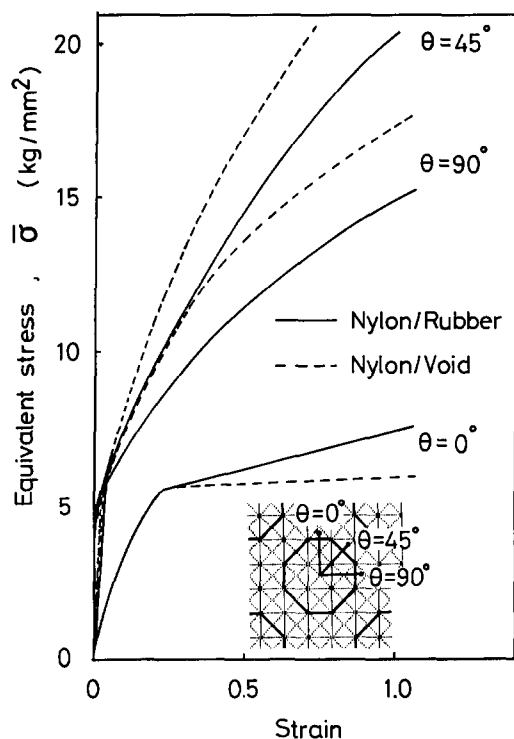


Figure 8 Stress evolved at three matrix elements indicated by the inset

in other words, the stress concentration is more uniform in the rubber system.

To discuss the fracture point, one has to establish a criterion for fracture. We simply assumed that the FEM element fractures when  $\bar{\sigma}$  exceeds the stress at break,  $\sigma_B$ , on the curve in Figure 4. In the FEM results shown in Figure 9, the elements for which  $\bar{\sigma}$  is larger than  $\sigma_B$  are densely shaded. There is no fractured element in the

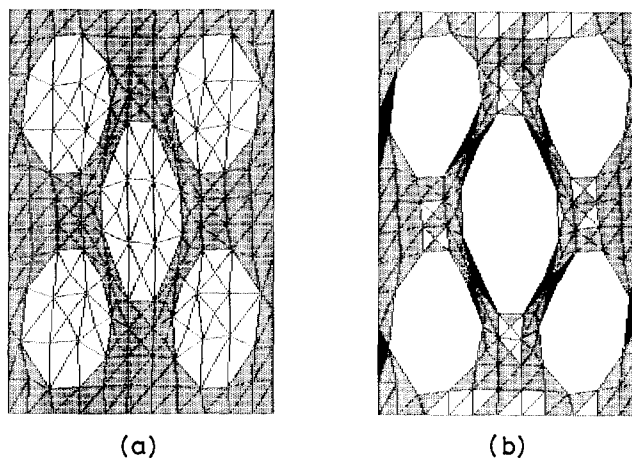


Figure 9 Stress concentration at  $\epsilon=0.5$  for (a) the nylon/rubber system and (b) the nylon/void system. Clear region,  $\bar{\sigma} < \sigma_y$ ; shaded region,  $\sigma_y < \bar{\sigma} < \sigma_B$ ; densely shaded region,  $\bar{\sigma} > \sigma_B$

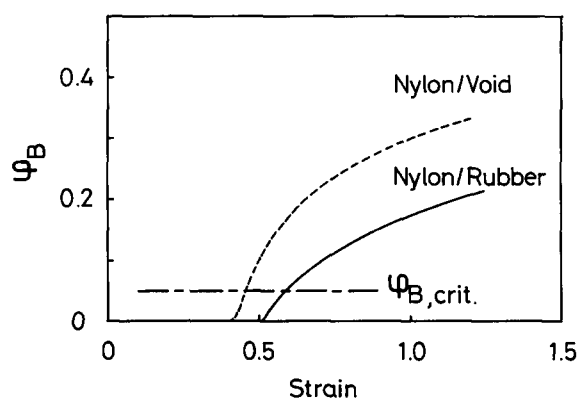


Figure 10 Number fraction of fractured elements,  $\phi_B$ , as a function of strain

rubber system (Figure 9a)\*. In contrast, many fractured elements have appeared in the void system (Figure 9b), again suggesting the more localized stress concentration to result in the coexistence of the unshaded, shaded and densely shaded regions. Note that the densely shaded regions in Figure 9b percolate with each other via voids throughout the system. This may correspond to a destructive crack. Such 'destructive percolation' was found to occur when the number fraction of fractured matrix elements,  $\phi_B$ , reaches  $\sim 0.05$  ( $\phi_{B/crit}$ , threshold fraction). Setting the above value of  $\phi_{B/crit}$ , the destructive percolation takes place at  $\epsilon=0.46$  and  $0.58$  for the void and rubber systems, respectively. This suggests that the strain at break is estimated to be larger for the rubber system than for the void system. Thus, the rubber inclusion seems to be more favourable for toughening also in terms of the strain at break. However it should be noted that the void inclusion is very effective for toughening. From the mechanical point of view, the interfacial debonding and cavitation may correspond to

\* In the nylon/rubber system, there is no fractured element in the nylon matrix or the rubber phase. By FEM analysis, the stress concentration in the rubber phase is highest at the centre of the rubber particle. The estimated  $\bar{\sigma}$  at the centre is  $0.668 \text{ kg mm}^{-2}$  at  $\epsilon=0.5$  and  $0.778 \text{ kg mm}^{-2}$  at  $\epsilon=0.7$ . These  $\bar{\sigma}$  values are far below  $\sigma_B$  of  $\text{EPR}$  ( $\sigma_B=2.15 \text{ kg mm}^{-2}$ ), by the stress-strain measurement. Hence, it is unnecessary to take into account cavitation in the rubber particle before the matrix fractures (Figure 10)

a transition from the rubber system to the void system. (The transition is represented by an arrow in *Figure 6*.) Even after the switch from the rubber system to the void system, there exists an excellent energy dissipation mechanism, although it is slightly less effective than in the case of no switching. Hence, void formation does not necessarily result in immediate fracture of the two-phase system and the toughening mechanism persists up to a certain strain level.

## CONCLUSIONS

The elastic-plastic analysis of the toughening mechanism in rubber-modified nylon was carried out by constructing a two-dimensional FEM model with five rubber inclusions. The rubber inclusion was found to induce massive yielding which would result in a large amount of energy dissipation. Similar analysis was carried out for the nylon/void system having the same geometry. It was shown that the void basically plays the same role as the rubber. The rubber inclusion was shown to provide a more favourable situation for toughening than the void, because the former deforms at a higher stress level, provides more massive yielding, and is preserved from

the development of destructive crack up to a higher strain level. From these results, it can be stated that a tougher material could be prepared when the interface is more strongly designed so that it is preserved from debonding, which corresponds to the transformation of the nylon/rubber system to the nylon/void system.

## ACKNOWLEDGEMENT

The authors thank Mr H. Urabe, Mitsubishi Kasei Co. Ltd, for kindly supplying the modified EPR.

## REFERENCES

- 1 Bucknall, C. B. 'Toughened Plastics', Applied Science Publishers, London, 1977
- 2 Wu, S. *J. Polym. Sci., Polym. Phys. Edn.* 1983, **21**, 699
- 3 Wu, S. *Polymer* 1985, **26**, 1855
- 4 Fukui, T., Urabe, H. and Inoue, T. *Kobunshi Ronbunshu* 1990, **47**, 315
- 5 Margolina, A. and Wu, S. *Polymer* 1988, **29**, 2170
- 6 Borggreve, R. J. M., Gaymans, R. J. and Eichenwald, H. M. *Polymer* 1989, **30**, 78
- 7 Hobbs, S. Y. and Dekkers, M. E. J. *J. Mater. Sci.* 1989, **24**, 1316
- 8 G'Sell, C. and Jonas, J. J. *J. Mater. Sci.* 1981, **16**, 1956